

# Liquid booster engine related TMF panel tests

Jörg Riccius\*, Gordan Thiede\* and Sebastian Weintritt\*

\*DLR Lampoldshausen

Im Langen Grund, D-74239 Hardthausen, Germany

## Abstract

The inner liner of the regeneratively cooled wall of the combustion chamber of a liquid booster engine is extremely loaded by the high temperature of the hot gas and the pressure difference between the coolant and the hot gas. A cyclic operation of such a chamber usually causes a low cycle fatigue failure of the wall structure. For the tests proposed in this paper, cyclic laser heating will be (as replacement for the hot gas) applied to an actively cooled small section of the hot gas wall of the real engine - the so called thermo-mechanical fatigue (TMF) panel. This manuscript contains a detailed description of the TMF test bench at DLR Lampoldshausen and shows the liquid booster nozzle throat TMF panel hardware. Finally the model, boundary conditions, and results of a coupled CFD analysis of the nitrogen flow inside the cooling channels and finite element analysis of the heat conduction inside the TMF panel structure are described.

## 1. Introduction

The strong demand for light-weight structures in space transportation systems leads to a close-to-the-limit design of all involved components – including the rocket engines. The combined thermally and mechanically induced (ratchetting caused) tensile rupture, low cycle fatigue (LCF) and creep failure of hot gas walls are the strongest limiting factors of the fatigue life of combustion chambers and expansion nozzles. The development and flight qualification of such components include structural and fatigue life analyses of the rocket engine's components and expensive full scale tests of the engine. Thermo-mechanical fatigue (TMF) panel tests can provide essential validation data for these numerical analyses and reduce the need for full scale tests considerably. Therefore, TMF panel tests have the potential of both, avoiding failure due to non-validated design analyses and saving full scale testing cost.

During a TMF panel test, only a small section of the hot gas wall of the real engine (the so called TMF panel) is tested. For this TMF panel, realistic (active) cooling conditions similar to the full scale rocket engine are chosen.

## 2. Components of the TMF panel test bench at DLR Lampoldshausen

### 2.1 The heating device of the TMF panel test bench

The key component of a TMF test bench is a heating device for the tested wall component. For medium heat flux applications, the following heating devices have been used:

- quartz tube radiant heaters without elliptical mirrors for flat nuclear rocket nozzle tube panels [1]
- quartz tube radiant heaters with elliptical mirrors for rotatory symmetric jet engine test specimens [2], [3].

However, combustion chambers of liquid propellant rocket engines are exposed to much higher heat flux densities compared to nozzle extension and jet engine structures. Consequently, realizing relevant environmental conditions inside a TMF test bench requires much higher power densities. Even a local combustion process under ambient pressure does not provide the high energy density which is necessary for this purpose.

Therefore, an optical heating device with a high energy density is required. The heating device of the TMF panel test facility at DLR Lampoldshausen was designed and built by DILAS Diodenlaser GmbH [4], [5]. The key technical parameters of this diode laser are given in Table 1.

Table 1: Key technical parameters of the diode laser of the TMF test bench at DLR Lampoldshausen

| Parameter  | Value                 |
|--|-----------------------|
| Wavelength   | 940 nm                |
| Maximum optical output power   | 11 kW                 |
| Distance from the optics module to the focal plane   | 415 mm                |
| Plateau cross section of the beam at the focal plane for the 8 MW/m <sup>2</sup> laser optics  | 19 mm x 51 mm         |
| Plateau cross section of the beam at the focal plane for the 28 MW/m <sup>2</sup> laser optics | 10 mm x 32 mm         |
| Homogeneity  | better than $\pm 5\%$ |
| Operational mode   | cw                    |

In order to indicate the intensity distribution of the laser beam at the focal plane, the infra-red laser light was transformed into visible light by fluorescent sheets as shown in Figure 1.

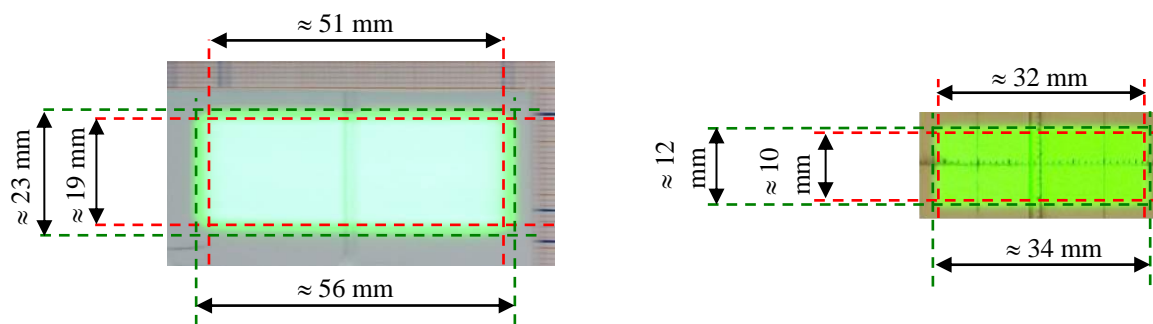


Figure 1: Visualization of the intensity distribution of the laser beam at the focal plane with an infra-red conversion screen for the 8 MW/m<sup>2</sup> optics (left) and for the newly acquired 28 MW/m<sup>2</sup> optics (right)

With the 19 mm x 51 mm laser optics, a typical heat flux of 8 MW/m<sup>2</sup> can be obtained in the plateau cross section of the laser beam as shown on the left-hand side of Figure 1. This optics is well suited for testing nozzle extension wall structures. Results of such tests were reported in [6] and [7].

With the newly acquired 10 mm x 32 mm laser optics, a typical heat flux of 28 MW/m<sup>2</sup> can be obtained in the plateau cross section of the laser beam as shown on the right-hand side of Figure 1. This is closer to the conditions equivalent to the heat flux in the nozzle throat cross section of a liquid booster engine than the 8 MW/m<sup>2</sup> of the 19 mm x 51 mm laser optics.

## 2.2 The TMF panel housing

In order to reduce water vapor condensation effects on the laser loaded side of the TMF panel wall material during the pre- and post-cooling phases of the TMF panel test, a TMF panel housing as shown in Figure 2 was designed.

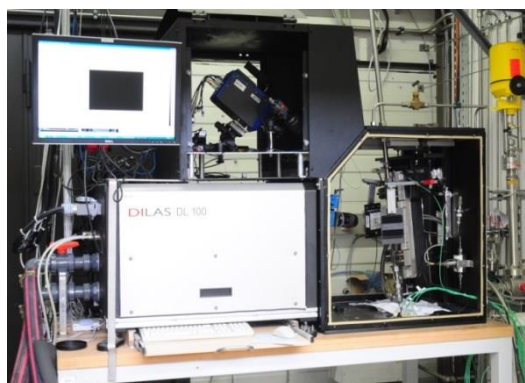


Figure 2: TMF panel test bench with laser head (left), infra-red camera (top) and TMF panel housing (side walls removed, right)

## 2.3 The measurement devices of the TMF panel test bench at DLR Lampoldshausen

### 2.3.1 The laser power meter

For the determination of the local heat flux into the TMF panel (which provides the heat flux distribution boundary condition for the thermal analysis of the TMF panel as shown on the right-hand side of Figure 8), the following values have to be measured:

- the absorption of the laser loaded surface at the laser wave length,
- the laser power distribution in the focal plane of the laser beam, and
- the total optical output power of the laser.

A special version of the PRIMES Power Monitor with an aperture of 250 mm x 50 mm as shown on the left-hand side of Figure 3 was used for the measurement of the laser power.



Figure 3: Devices for characterizing the laser beam: laser power meter (left) and laser beam profiler (right)

For laser power values between 1 kW and 12 kW, the measurement uncertainty of the system is better than  $\pm 2\%$  of the measured value [8].

### 2.3.2 The laser beam profiler

The distribution of the laser power in the focal plane of the laser beam was determined by the PRIMES laser beam monitor BM100 (as shown on the right-hand side of Figure 3) with a resolution of 256 x 128 pixels and a measurement uncertainty of smaller than  $\pm 3\%$  of the measured value.

### 2.3.3 The laser wave length pyrometer

The absorption of the laser loaded surface at elevated temperatures was measured by a pyrometer with an identical wavelength as the laser wavelength. This high end transfer standard pyrometer IMPAC IS12-TSP is shown on the left-hand side of Figure 4. Temperatures can be measured with this pyrometer with an uncertainty of  $\pm 0.15\%$  of the measured value  $\pm 1$  °C at a measurement range between 430 °C and 1300 °C. In addition, a narrow band pass filter with a center wavelength of 940 nm  $\pm$  4 nm and a half width of 20 nm  $\pm$  4 nm was used.



Figure 4: Devices for the determination of the emissivity of the TMF panel coating during pre-tests: laser wavelength pyrometer (left) and infra-red camera (right)

### 2.3.4 The infra-red camera

The 2d thermal field at the laser loaded side of the TMF panel was measured by an infra-red camera (as shown on the right-hand side of Figure 4) with a resolution of 640 x 512 pixel, a maximum acquisition rate of 100 Hz and a measurement range of 300 °C to 1500 °C. Related to a black body, the measurement uncertainty of this infra-red

camera is lower than  $\pm 1\%$  of the measured temperature value. To avoid a possible influence of reflected infra-red laser radiation to the temperature measurement, a narrow band pass filter with a wavelength of  $3.99 \mu\text{m}$  was used.

### 2.3.5 The deformation measurement systems

During the TMF test, the deformation of the TMF panel will be measured by an image correlation [9] system as shown on the left-hand side of Figure 5. In order to obtain the lowest possible measurement uncertainty, a system consisting of two 16 megapixel cameras was selected. This measurement system requires the application of small speckle marks to the surface of the TMF panel and allows for the measurement of 3 component ( $u_x$ ,  $u_y$ ,  $u_z$ ) 2d displacement fields on the surface of the TMF panel before, during and after the laser loading. After the completion of the TMF test, the surface geometry and the cross section of the TMF panel will be assessed by a digital microscope as shown on the right-hand side of Figure 5. The out-of-plane component of the surface geometry will be determined by the “depth from defocus” technology with a 500 nm resolution step motor.



Figure 5: Devices for the measurement of the deformation of the TMF panel during the TMF test: stereo camera system (left) and after the TMF test: digital microscope (right)

## 3. Pre-test characterization of the TMF laser beam in its focal plane

A laser beam profiler as shown on the right-hand side of Figure 3 was used for the characterization of the beam of the TMF laser in its focal plane. The measurement shown in Figure 6 is related to a perpendicular cross section of the laser beam.

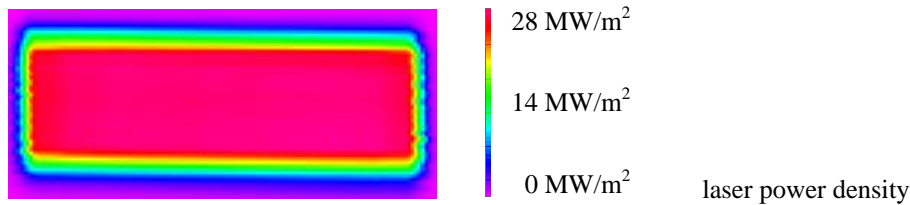


Figure 6: Profile of the TMF laser in its focal plane for an optical output laser power of 11 kW

## 4. The liquid booster nozzle throat TMF panel hardware

Cooling channel dimensions almost completely identical to the ones described in [10] were assumed for the liquid booster nozzle throat TMF panel. These geometric parameters are summarized in Table 2.

Table 2: Cooling channel parameters assumed for the nozzle throat cross section of the liquid booster nozzle throat TMF panel

| Width of the cooling channels | Height of the cooling channels | Angle between adjacent cooling channels | Total number of cooling channels in the TMF panel | Thickness of the laser loaded wall | Curvature radius of the laser loaded surface |
|-------------------------------|--------------------------------|---|---|------------------------------------|--|
| 1.3 mm                        | 9.0 mm                         | 1.0 °                                   | 7   | 1.0 mm                             | 130 mm                                       |

In contrary to all other TMF panels tested at DLR Lampoldshausen (containing planar laser loading surfaces), the laser loaded surface of the liquid booster nozzle throat TMF panel has a cylindrical surface in order to obtain an accumulation of tensile deformation in the centerline cooling channel of the liquid booster nozzle throat TMF panel. Photographs of the TMF panel without and with coating are shown in Figure 7.



Figure 7: The liquid booster nozzle throat TMF panel made from CuCrZr in the laser-loading section (left) and coated TMF panel (right)

The absorption and emissivity increasing coating on the laser-loaded side of the TMF-panel as shown on the right-hand side of Figure 7 will ensure:

- Avoiding as much as possible reflected laser light which would damage TMF measurement devices such as the ones shown at the right-hand side of Figure 4 and on the left-hand side of Figure 5. Without the TMF panel coating, the pure CuCrZr surface of the TMF panel (shown on the left-hand side of Figure 7) would act almost like a mirror at the spectral range of the laser (940 nm).
- Increasing the accuracy of the optical temperature measurement. Without the TMF panel coating, the low emissivity of the pure CuCrZr surface would increase strongly during the TMF test due to an oxidation of its laser-loaded surface as well as due to a straining-caused roughness increase of the laser loaded surface.
- Application of high-contrast speckle marks on the surface of the TMF panel in order to measure the surface deformation by a successive application of a stereo-camera system and some image correlation software.

## 5. Pre-test determination of the TMF panel coolant mass flow rate

In order to determine the mass flow rate of gaseous nitrogen ( $\text{GN}_2$ ) which is necessary to obtain the intended maximum TMF panel temperature of 900 K while the TMF laser is running with an optical output power of 10 kW, the following coupled stationary analyses were performed [11]:

- Computational Fluid Dynamics (CFD) analysis of the (TMF test bench provided)  $\text{GN}_2$  flow through the 7 cooling channels of the TMF panel (RANS, SST turbulence model)
- Thermal finite element (FE) analysis of the heat conduction in the TMF panel structure (made from CuCrZr)

For symmetry reasons, only a half of the TMF panel was modelled.

### 5.1 Boundary conditions

The single parameter boundary conditions for this coupled CFD and FE analysis are summarized in Table 3.

Table 3: Boundary conditions for the coupled CFD analysis of the  $\text{GN}_2$  flow and for the thermal FE analysis of the TMF panel

| $\text{GN}_2$ inlet temperature | $\text{GN}_2$ outlet pressure | Roughness of the cooling channel surfaces in axial direction | Total mass flow rate through all of the 7 cooling channels |
|---------------------------------|-------------------------------|--|--|
| 160 K                           | 5 MPa                         | 1,75 $\mu\text{m}$   | 225 g/s  |

The 2d heat flux boundary condition for the thermal FE analysis of the TMF panel is visualized in Figure 8. It represents the power distribution of the TMF laser in its focal plane as measured with the laser beam profiler (as

shown in the right-hand side of Figure 3) multiplied by the absorption coefficient of the TMF panel coating at the spectral range of the laser (940 nm) at the test temperature (900 K).

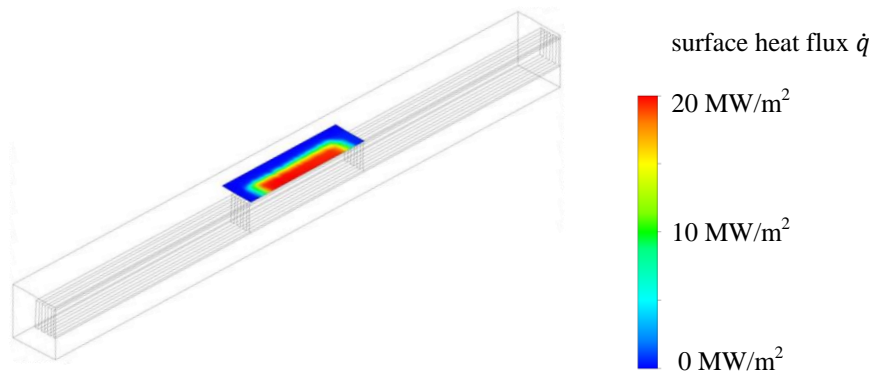


Figure 8: Wireframe model of a half liquid booster nozzle throat TMF panel including a visualization of the heat flux boundary condition at an angle of 5° for the thermal analysis of this TMF panel.

## 5.2 CFD and FE meshes

The CFD and FE meshes of the liquid booster nozzle throat TMF panel are shown in Figure 9.

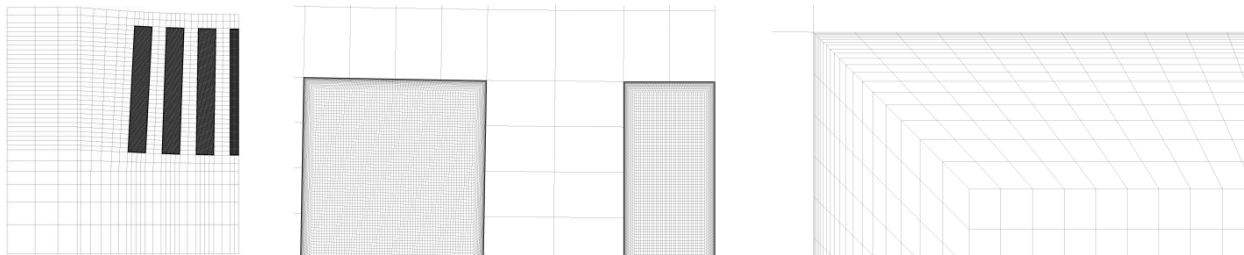


Figure 9: CFD and FE meshes in the cross section of the TMF panel: full mesh (left) and gradually magnified meshes, showing the mesh refinement in the boundary layer regions of the cooling channels (middle and right)

## 5.3 Results of the coupled CFD and thermal FE analysis

The results of the thermal analysis shown in Figure 10 indicate that the total mass flow rate of 225 g/s (as given on the right-hand side of Table 3) will indeed result in the intended maximum temperature of the TMF panel of 900 K when a total laser output power of 10 kW is applied.

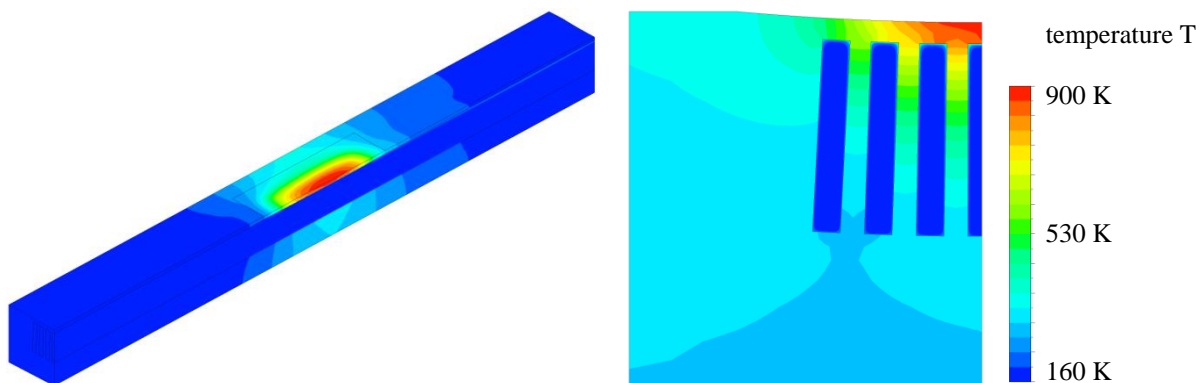


Figure 10: Temperature distribution in the liquid booster nozzle throat TMF panel as result of the coupled CFD analysis of the GN<sub>2</sub> flow through the cooling channels and the FE analysis of the heat conduction in the TMF panel wall structure: 3d visualisation (left) and in the center cross section of the TMF panel (right)

## 6. Outlook

Whereas in this manuscript just the preparation of liquid booster nozzle throat TMF panel tests is shown, the results of these TMF panel tests will finally provide realistic validation data for:

- coupled CFD analyses of coolant flows inside asymmetrically heated, high aspect ratio cooling channels and thermal FE analyses of actively cooled liquid rocket engine structures at realistic hot-run temperatures, and
- structural and fatigue life analyses of actively cooled structures of liquid rocket engines at realistic thermal and mechanical loading.

## 7. Acknowledgement

The liquid booster engine related TMF panel tests proposed in this manuscript will be performed in the framework of the DLR-internal AKIRA project [12].

## References

- [1] A. E. Carden, D. G. Harman and E. A. Franco-Ferreira. 1966. Thermal fatigue analysis of a cryogenically cooled rocket nozzle. In: *Southeastern Symposium in Missiles and Aerospace Vehicles Sciences*, Huntsville, Alabama.
- [2] B. Baufeld and M. Bartsch. 2002. Temperature Measurement in Thermal Gradient Mechanical Fatigue Testing of Material Systems with Coatings. In: *Advanced Materials and Processes for Gas Turbines*. p. 75 – 82.
- [3] M. Bartsch, B. Baufeld and M. Heinzlmann. 2006. CMSX-4 with Thermal Barrier Coating under Thermal Gradient Mechanical Fatigue. In: *9th International Conference on Fatigue*.
- [4] G. Overton. 2005. Laser-Beam Shaping: Diode-laser system yields 11 kW homogenized output. *Laser Focus World*, Volume 43, Issue 5
- [5] B. Köhler, A. Noeske, T. Kindervater, A. Wessollek, T. Brand und J. Biesenbach. 2007. 11 kW direct diode laser system with homogenized 55 x 20 mm<sup>2</sup> Top-Hat intensity distribution. In: *Photonics West*.
- [6] A. Gernoth, J. R. Riccius and S. Schlechtriem. 2011. Optical heating, thermography and deformation measurement of nozzle wall structures. In: *49th AIAA Aerospace Sciences Meeting*, Orlando.
- [7] A. Gernoth, D. Greuel and S. Schlechtriem. 2011. Experimental Validation of numerical simulations of flows in cooling channels of liquid rocket engines. In: *4th European Conference for Aerospace Sciences (EUCASS)*. St. Petersburg, Russia.
- [8] V. Brandl, K. Hänsel, R. Kramer und H. Schwede. 2003. Calibration of Laser Power Meters in the Multikilowatt Range. In: *Laser Beam Characterization, Instruments and Standard Test Procedures for Laser Beam and Optics Characterization. CHOCLAB II. Eureka project EU-2359*. VDI Technology Center.
- [9] M. A. Sutton, J.-J. Orteu and H. W. Schreier. 2009. *Image Correlation for Shape, Motion and Deformation Measurements: Basic Concepts, Theory and Applications*. Springer-Verlag GmbH.
- [10] D. Kuhl, J. Riccius and O. J. Haidn. 2002. Thermomechanical Analysis and Optimization of Cryogenic Liquid Rocket Engines. *Journal of Propulsion and Power*. Vol. 18, No. 4.
- [11] S. Weintritt. 2017. Modellierung und Durchführung gekoppelter Strömungs- und Strukturberechnungen (FSI) von TMF-Panel-Experimenten mit zyklischer Laserbelastung. Master Thesis. DLR Lampoldshausen.
- [12] A. Kopp, M. Sippel, N. Darkow, J. Gerstmann, S. Krause, D. Stefaniak, J. Riccius, T. Thiele, T. Reimer, A. Kolbe, K. Schnepfer and L.E. Briese. 2017. Forschung an Systemen und Technologien für Wiederverwendbare Raumtransportsysteme im DLR-Projekt AKIRA. 66. *Deutscher Luft- und Raumfahrtkongress*, Munich, Germany